Optimization of the tilt angles in reflection-mode ptychographic reconstructions by leveraging the flexibility of automatic differentiation-based modeling

Senhorst, Sander; Shao, Yifeng; Weerdenburg, Sven; Horsten, Roland; Porter, Christina; Coene, Wim

DOI
10.1117/12.3027947

Publication date
2024

Document Version
Final published version

Published in
UV and Higher Energy Photonics

Citation (APA)
Senhorst, S., Shao, Y., Weerdenburg, S., Horsten, R., Porter, C., & Coene, W. (2024). Optimization of the tilt angles in reflection-mode ptychographic reconstructions by leveraging the flexibility of automatic differentiation-based modeling. In G. Lerondel, Y.-H. Cho, & A. Taguchi (Eds.), *UV and Higher Energy Photonics: From Materials to Applications 2024* Article 1311503 (Proceedings of SPIE - The International Society for Optical Engineering; Vol. 13115). SPIE. https://doi.org/10.1117/12.3027947

Optimization of the tilt angles in reflection-mode ptychographic reconstructions by leveraging the flexibility of automatic differentiation-based modeling

Sander Senhorst[a], Yifeng Shao[a], Sven Weerdenburg[a], Roland Horsten[a], Christina Porter[b], and Wim Coene[a,b]

[a]Department of Imaging Physics, Delft University of Technology, Lorentzweg 1, 2628 CJ Delft, The Netherlands,
[b]ASML Netherlands B.V., De Run 6501, 5504 DR Veldhoven, The Netherlands.,

ABSTRACT

Ptychography as a means of lensless imaging is used in wafer metrology applications using Extreme Ultraviolet (EUV) light, where use of high quality optics is out-of-scope. To obtain sufficient diffraction intensity, reflection geometries with shallow (ca. 20 degrees) grazing incidence angles are used, which require re-sampling the diffraction data in a process called tilted plane correction (TPC). The tilt angle used for TPC is conventionally obtained through either experimentally tricky calibration, manual estimation based on diffraction pattern symmetry, although computational approaches are emerging. In this work we offer an improved numerical optimization approach as an alternative to TPC, where we use the flexibility offered by our Automatic Differentiation (AD)-based ptychography approach to include the data resampling into the forward model to learn the tilt angle. We demonstrate convergence of the approach across a range of incidence angles on simulated and experimental data obtained on an EUV beamline with either a high-harmonic generation (HHG)-based or a visible light source.

Keywords: Reflection Ptychography, Automatic differentiation, Tilted-plane correction, Extreme Ultraviolet metrology

1. INTRODUCTION

In applications where use of high-quality, diffraction-limited optics is out-of-scope, lensless imaging can provide a means of generating high-resolution images without the need for diffraction-limited imaging optics. The imaging of patterned nanostructures using extreme ultraviolet (EUV) radiation is one such application area.[1–5] Ptychography is a means of lensless imaging, where a coherent probe beam is scanned across a sample through several scanning positions, while at every position the resulting diffraction pattern is measured. When imaging nanostructures on thick, opaque substrates using ptychography, one must make use of a reflection geometry, since the substrate absorbs all light in the transmission direction. For the specific case of EUV ptychography, generation of sufficient diffracted intensity requires shallow incidence angles between 70 and 80 degrees with respect to the surface normal. These shallow incidence angles provide additional challenges, for example the curvature of the measured diffraction pattern due to the rotation between the sample and the detector planes.[6]

The curved diffraction patterns are traditionally processed using 'tilted plane correction' (TPC),[2,7–9] where the measured diffraction patterns are straightened by interpolating the curved coordinates onto rectilinear coordinates. This process is sensitive to the parameters used for the transformation; the incidence angle(s) and propagation distance, which are not always calibrated with sufficient accuracy to provide ptychographic reconstructions without artifacts. When more accurate calibration is experimentally not feasible, one may attempt to use symmetry in the diffraction pattern as a means of manually estimating the correct parameters, but this assumes real-valued samples and will be increasingly inaccurate as the incident probe NA increases. To provide a more robust, reproducible approach to ptychographic reconstructions, a new methodology is required.

Further author information: (Send correspondence to Sander Senhorst)
Sander Senhorst: E-mail: s.senhorst@tudelft.nl

UV and Higher Energy Photonics: From Materials to Applications 2024, edited by Gilles Lérondel, Yong-Hoon Cho, Atsushi Taguchi, Proc. of SPIE Vol. 13115, 1311503
© 2024 SPIE · 0277-786X · doi: 10.1117/12.3027947

Recently, there have been developments into computational correction of the diffraction pattern tilt, by the name of aPIE.[10] This is a valuable demonstration of the feasibility of algorithmic correction of the tilted diffraction, however only limited incidence angles and a small numerical aperture (NA) were considered. Moreover, the precision of the solution was significantly lower for experimental beams without the use of a diffuser.

In this work,[11] we will demonstrate a novel approach to algorithmic correction of the tilting transformation. We will leverage the flexibility of optimization by automatic differentiation (AD)-based[12] gradient descent to include the effects of tilted propagation into the forward prediction of the diffraction patterns, in contrast to the backwards correction of the tilted diffraction patterns before reconstruction. This approach allows us to jointly optimize for all parameters of the ptychographic model on a per-iteration basis.

2. METHODS

In the ptychographic forward model, the interaction between the coherent complex probe beam $P(x,y)$ of wavelength λ and the complex-valued sample reflection function $O(x,y)$ is modeled as a simple multiplication to give the exit field U_e at the sample plane

$$U_e(x,y) = P(x,y)O(x,y)\exp\left[ikx\sin\phi_{i,y}\right], \tag{1}$$

where $k = \frac{2\pi}{\lambda}$ and $\phi_{i,y}$ the angle of incidence with respect to the surface normal. The propagation of the exit field from the sample to the field at the detector U_d is given by the standard Fraunhofer propagation integral, but interpolated onto transformed coordinates[13]

$$U_d\left(x',y'\right) = \iint U_e(x,y)\exp\left[i(x\xi_x + y\xi_y)\right]dxdy\bigg|_{\boldsymbol{\xi}_\perp = f\left(\boldsymbol{\xi}'_\perp\right)}, \tag{2}$$

where $\xi_\perp$ and $\xi'_\perp = \left(\frac{kx'}{z'_d}, \frac{ky'}{z'_d}\right)$ are the Fourier coordinates in the sample and detector coordinate systems respectively. The function f transforms the far-field coordinates of the parallel plane towards the rotated detector:

$$\boldsymbol{\xi}_\perp = f(\boldsymbol{\xi}'_\perp) = \begin{bmatrix} R_{00} & R_{01} & R_{02} \\ R_{10} & R_{11} & R_{12} \end{bmatrix} \begin{bmatrix} \xi'_x \\ \xi'_y \\ \sqrt{k^2 - \xi'^2_x - \xi'^2_y} \end{bmatrix}, \tag{3}$$

where $R_{i,j}$ are the components of a three-dimensional rotation matrix describing the rotation between the sample and detector coordinate systems. We assume elastic scattering to find ξ_z using the Ewald Sphere condition $|\boldsymbol{\xi}|^2 = k^2$. The rotation matrix and rotation angles are defined as

$$\begin{aligned} R(\phi_x,\phi_y,\phi_z) = R_x(\phi_x)R_y(\phi_y)R_z(\phi_z) &= \begin{bmatrix} R_{00} & R_{01} & R_{02} \\ R_{10} & R_{11} & R_{12} \\ R_{20} & R_{21} & R_{22} \end{bmatrix} \\ &= \begin{bmatrix} 1 & 0 & 0 \\ 0 & \cos\phi_x & \sin\phi_x \\ 0 & -\sin\phi_x & \cos\phi_x \end{bmatrix} \begin{bmatrix} \cos\phi_y & 0 & \sin\phi_y \\ 0 & 1 & 0 \\ -\sin\phi_y & 0 & \cos\phi_y \end{bmatrix} \begin{bmatrix} \cos\phi_z & \sin\phi_z & 0 \\ -\sin\phi_z & \cos\phi_z & 0 \\ 0 & 0 & 1 \end{bmatrix}. \end{aligned} \tag{4}$$

Fig. 1a schematically shows the definition of the rotation angles. The detector measures $I_d = |U_d|^2$ on a square grid of pixels in the primed coordinates. The traditional TPC approach would transform these primed coordinates into the non-primed coordinates of the plane parallel to the sample and subsequently interpolate I_d onto a square grid in the non-primed coordinates. These are the diffraction patterns that are to be used for ptychographic reconstructions. In our approach, we interpolate the other way around; we model the probe and object in rectilinear coordinates in the non-primed frame and interpolate the diffraction pattern resulting from these samples onto the primed frame. The interpolation is an integral part of the reconstruction process

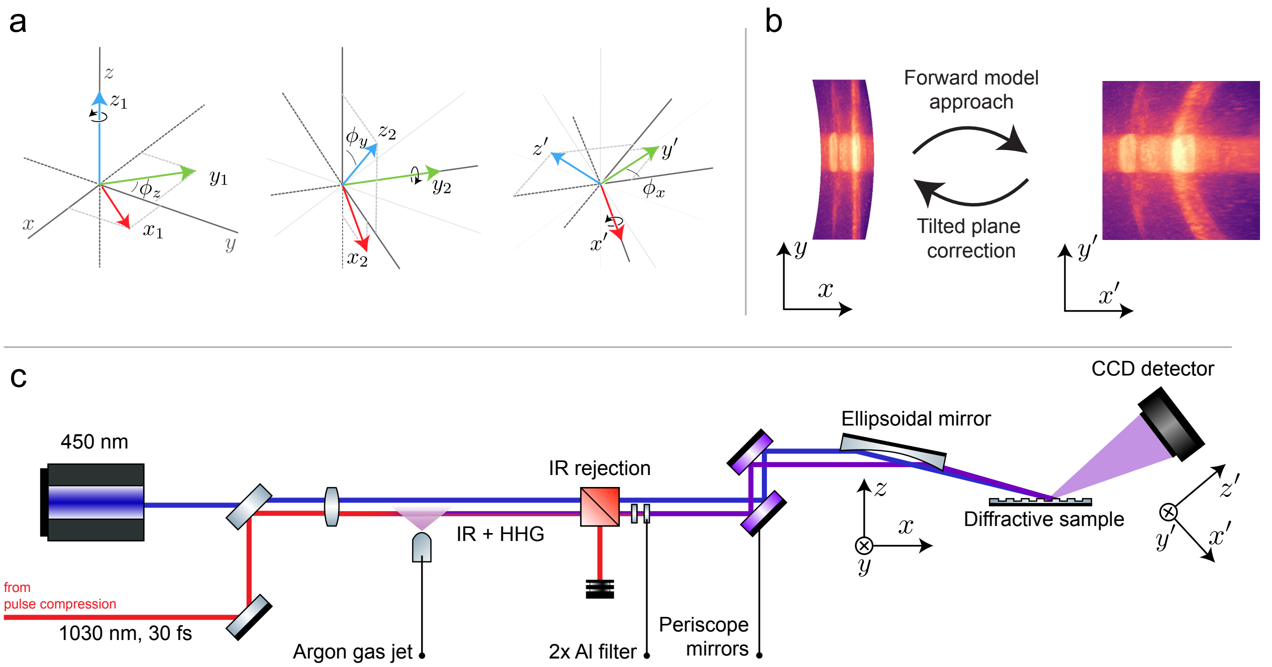

Figure 1. a) The definition of the rotation angles. First, we rotate by ϕ_z around the z-axis, then ϕ_y around the newly rotated y_1-axis, then by ϕ_x around the newly rotated x_2-axis, to obtain the new (x', y', z') coordinate system. b) The difference between the forward model approach and the tilted plane correction approach. In the latter, the measured diffraction patterns, shown on the right, are interpolated onto rectilinear coordinates in the non-primed frame. This approach adjusts the curved lines to straight lines in the non-primed coordinates. On the other hand, the forward model approach first computes a diffraction pattern in the non-primed coordinates. This diffraction pattern is then interpolated on the coordinates of the measured diffraction pattern. c) A schematic of the experimental setup used for ptychographic imaging. From the left, the input light consisted of either a 450 nm blue laser or a pulsed infrared (IR) laser. In the latter case, the light is focused close to a Argon gas jet to produce high harmonic generation (HHG) extreme ultraviolet (EUV) radiation, after which the IR beam is filtered out. A periscope consisting of two multilayer mirrors select the 17.5 nm wavelength from the generated HHG spectrum, while the 450 nm illumination is simply reflected. An ellipsoidal mirror then focuses the light onto the sample, after which the reflected light is measured by a CCD detector.

and is computed using the same AD framework as the remainder of the model. We make use of bilinear interpolation, which takes a weighted sum of all pixels surrounding a sample. Due to the weighting, a slight change in the coordinates produces a slight change in the output of the interpolation operation, in other words: the interpolation operation is differentiable with respect to the input coordinates and, by extension, to the tilt angles ϕ_x, ϕ_y and ϕ_z. This means that the gradient of the tilt angle with respect to the loss function may now be computed as if they were any other parameter of the optimization process.

3. RESULTS

To validate the proposed method, it was applied to two datasets, one using 450 nm illumination and one using 17.5 nm EUV illumination. Both experiments were recorded on the same beamline, which may be switched between a 450 nm illumination and EUV illumination. The experimental setup used is schematically shown in Fig. 1c. For more details on the setup, we refer to Ref.[14] In the 450 nm experiments, we imaged a 1997 Toshiba integrated circuit under an incidence angle of $70^\circ \pm 1^\circ$ with respect to the surface normal. This, combined with the detection NA of 0.3 resulted in visibly curved diffraction patterns, as can be seen in Fig. 1b. The proposed tilt optimization approach was applied to this dataset. Tilt optimization was enabled after 10 iterations where the tilt angles were constant to improve stability. As can be seen in Fig 2a-b, optimization of the incidence angle visibly improved contrast if an initial error of 2° was introduced. To test the convergence behavior, the newly

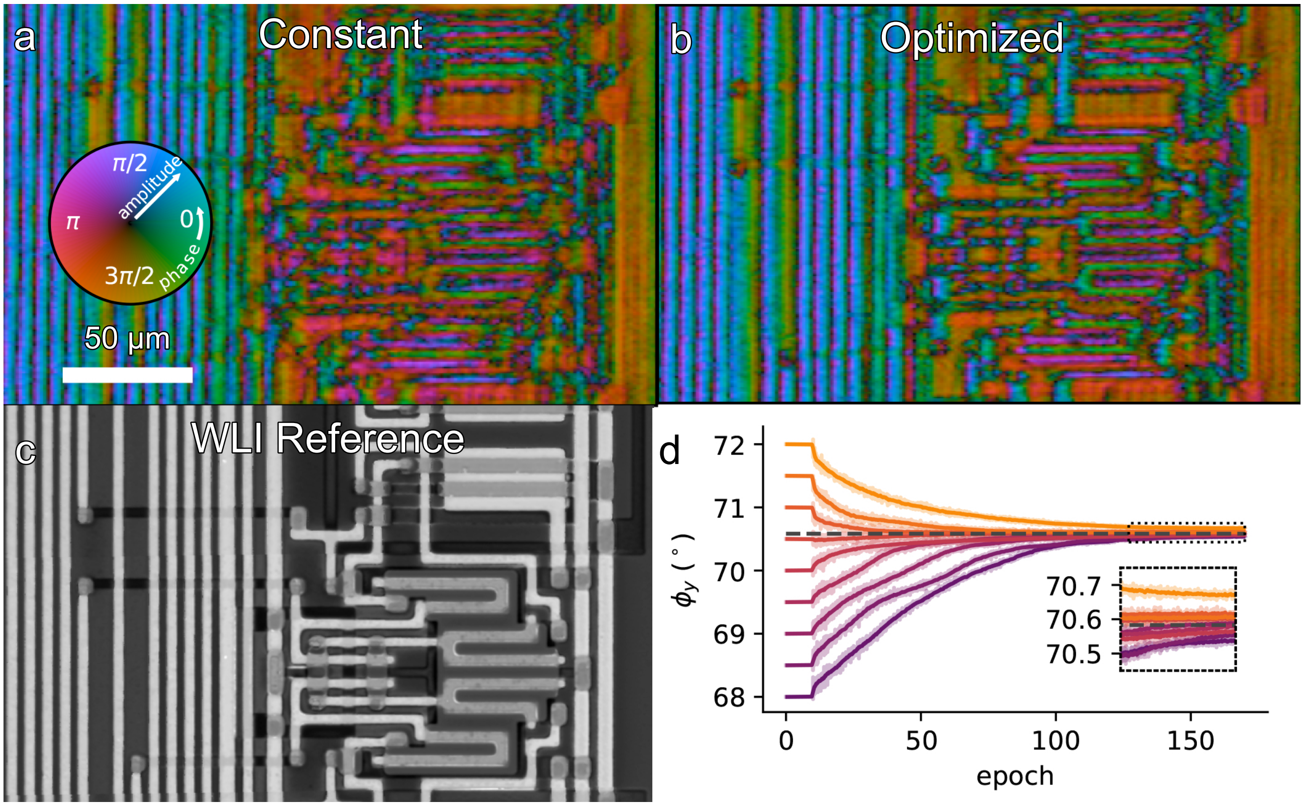

Figure 2. a,b) A region of interest of the complex-valued reconstructed sample obtained on the 450 nm illumination datasets. The initial tilt angle was set to 68° with respect to the normal and was either kept constant (a) or optimized (b). The phase contrast was enhanced by increasing the brightness of low-amplitude signals, as is reflected in the colormap. c) A reference image taken by a white-light interferometer (WLI), showing height contrast. d) The convergence behavior of the tilt angle ϕ_y for various initial guesses.

proposed method was applied to the dataset for a range of initial angles ϕ_y between 68 and 72°, the other angles were initialized at 0. As can be seen in 2d, the newly proposed approach could reliably converge for this range of initial angles. The other tilt angles all remained within 0.5° of their initial values.

The approach was additionally applied to datasets with EUV illumination. The sample was a 20 nm height gold Siemens star patterned on a silicon substrate. As is shown in Fig. 3a, the imposed tilt angle error of approximately 2° resulted in visible artifacts in the Siemens star. In Fig. 3b we observe that this artifact is displaced towards the higher spatial frequencies upon enabling tilt optimization. The artifact can be interpreted as a demonstration of internal inconsistency in the reconstruction, as the outer spokes are 'out of phase' with the inner spokes. By pixel-wise multiplication with a scanning electron microscope (SEM) reference image of the same region, also absolute likeness to the sample could be visualized. The Siemens Star periodicity produces Moiré patterns if there is an error between the reconstruction and the reference. These Moire patterns were very visible in the case where tilt training was not enabled (Fig. 3c), and again nearly disappeared when training was enabled (Fig. 3d).

4. CONCLUSION

We have introduced a new approach for reflection ptychography, where the forward model predicting the diffraction patterns incorporates the effects of tilted propagation. The approach was validated on datasets using 450 nm and EUV illumination. The results show that tilt training can reliably converge for large tilt angles. Additionally, our approach is able to suppress tilt-induced artifacts in the reconstruction, and increases the absolute likeness to the sample.

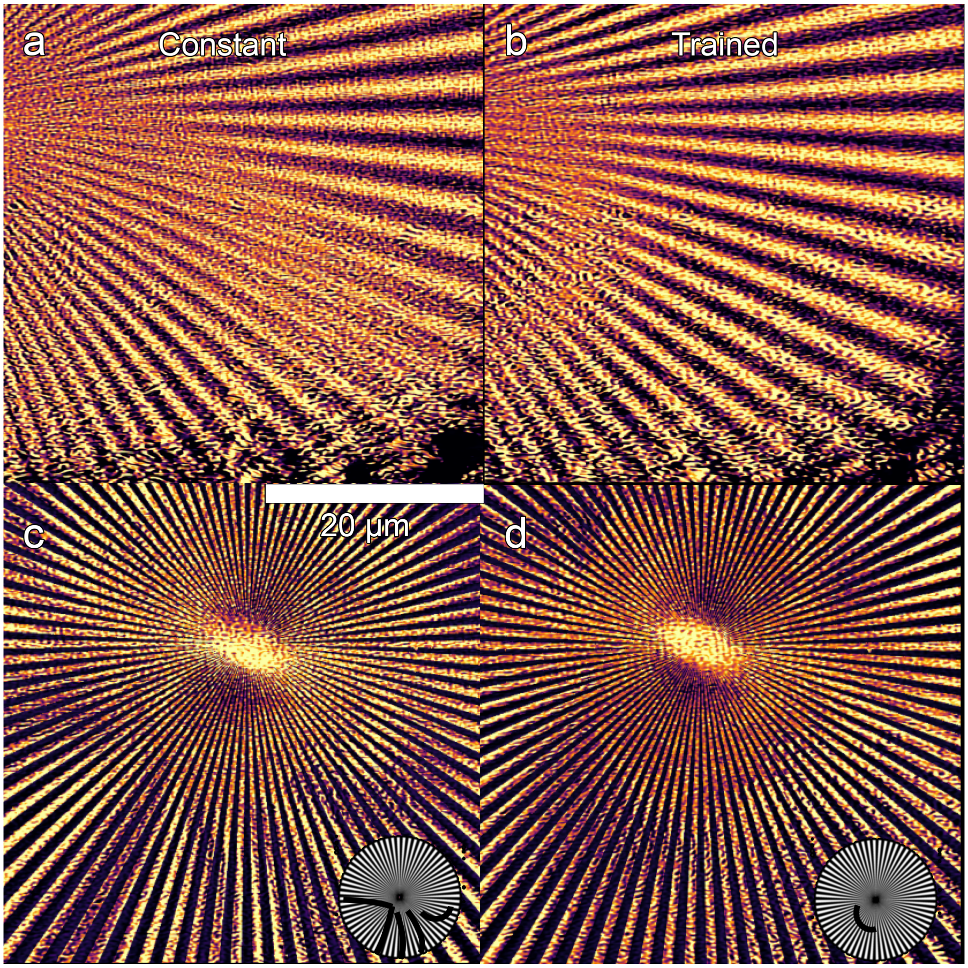

Figure 3. a, b) The reconstructed amplitude of the sample, showing an example artifact generated by reconstructing the EUV dataset with a constant (a) or optimized (b) tilt angle $\phi_y = 68^\circ$. As can be seen, the artifact has moved inwards toward the higher spatial frequencies of the Siemens star. c,d) The reconstructed sample with a constant (c) or trained (d) tilt angle after multiplying pixel-by-pixel with the SEM reference. Due to the periodic nature of the Siemens star, Moiré patterns appear wherever the reconstruction is 'out of phase' with the reference. The multiple Moiré pattern streaks present in the constant case (c) disappear after training. The inset indicates where the streaks occur.

ACKNOWLEDGMENTS

The authors wish to thank the funding agencies; the Dutch government Holland High Tech / TKI project with project partners ASML and DEMCON. Additionally, we wish to thank M. Dubbelman for his help in generating the white-light interferometry reference images.

REFERENCES

[1] Sandberg, R. L., Paul, A., Raymondson, D. A., Hädrich, S., Gaudiosi, D. M., Holtsnider, J., Tobey, R. I., Cohen, O., Murnane, M. M., Kapteyn, H. C., Song, C., Miao, J., Liu, Y., and Salmassi, F., "Lensless diffractive imaging using tabletop coherent high-harmonic soft-X-ray beams," *Physical Review Letters* **99**, 098103–098103 (Aug. 2007). Publisher: American Physical Society.

[2] Gardner, D. F., Zhang, B., Seaberg, M. D., Martin, L. S., Adams, D. E., Salmassi, F., Gullikson, E., Kapteyn, H., and Murnane, M., "High numerical aperture reflection mode coherent diffraction microscopy using off-axis apertured illumination," *Optics Express* **20**, 19050 (Aug. 2012).

[3] Esashi, Y., Jenkins, N. W., Shao, Y., Shaw, J. M., Park, S., Murnane, M. M., Kapteyn, H. C., and Tanksalvala, M., "Tabletop extreme ultraviolet reflectometer for quantitative nanoscale reflectometry, scatterometry, and imaging," *Review of Scientific Instruments* **94**, 123705 (Dec. 2023). Publisher: AIP Publishing.

[4] Odstřcil, M., Lebugle, M., Guizar-Sicairos, M., David, C., and Holler, M., "Towards optimized illumination for high-resolution ptychography," *Optics Express, Vol. 27, Issue 10, pp. 14981-14997* **27**, 14981–14997 (May 2019). Publisher: Optica Publishing Group.

[5] Eschen, W., Loetgering, L., Schuster, V., Klas, R., Kirsche, A., Berthold, L., Steinert, M., Pertsch, T., Gross, H., Krause, M., Limpert, J., and Rothhardt, J., "Material-specific high-resolution table-top extreme ultraviolet microscopy," *Light: Science & Applications 2022 11:1* **11**, 1–10 (Apr. 2022). Publisher: Nature Publishing Group.

[6] Patorski, K., "Fraunhofer Diffraction Patterns of Titled Planar Objects," *Optica Acta: International Journal of Optics* **30**, 673–679 (May 1983). Publisher: Taylor & Francis _eprint: https://doi.org/10.1080/713821241.

[7] Marathe, S., Kim, S. S., Kim, S. N., Kim, C., Kang, H. C., Nickles, P. V., and Noh, D. Y., "Coherent diffraction surface imaging in reflection geometry," *Optics Express* **18**, 7253–7262 (Mar. 2010). Publisher: Optica Publishing Group.

[8] Porter, C. L., Tanksalvala, M., Gerrity, M., Miley, G., Zhang, X., Bevis, C., Shanblatt, E., Karl, R., Murnane, M. M., Adams, D. E., and Kapteyn, H. C., "General-purpose, wide field-of-view reflection imaging with a tabletop 13 nm light source," *Optica* **4**, 1552 (Dec. 2017).

[9] Seaberg, M. D., Zhang, B., Gardner, D. F., Shanblatt, E. R., Murnane, M. M., Kapteyn, H. C., and Adams, D. E., "Tabletop nanometer extreme ultraviolet imaging in an extended reflection mode using coherent Fresnel ptychography," *Optica, Vol. 1, Issue 1, pp. 39-44* **1**, 39–44 (July 2014). Publisher: Optica Publishing Group.

[10] Beurs, A. d., Loetgering, L., Herczog, M., Du, M., Eikema, K. S. E., and Witte, S., "aPIE: an angle calibration algorithm for reflection ptychography," *Optics Letters, Vol. 47, Issue 8, pp. 1949-1952* **47**, 1949–1952 (Apr. 2022). Publisher: Optica Publishing Group.

[11] Senhorst, S., Shao, Y., Weerdenburg, S., Horsten, R., Porter, C., and Coene, W., "Mitigating tilt-induced artifacts in reflection ptychography via optimization of the tilt angles," Submitted for publication (Aug. 2024).

[12] Kandel, S., Maddali, S., Allain, M., Hruszkewycz, S. O., Jacobsen, C., and Nashed, Y. S. G., "Using automatic differentiation as a general framework for ptychographic reconstruction," *Optics Express* **27**, 18653–18672 (June 2019). Publisher: Optica Publishing Group.

[13] Wyrowski, F., Schimmel, H., and Matsushima, K., "Fast calculation method for optical diffraction on tilted planes by use of the angular spectrum of plane waves," *JOSA A, Vol. 20, Issue 9, pp. 1755-1762* **20**, 1755–1762 (Sept. 2003). Publisher: Optica Publishing Group.

[14] Shao, Y., Weerdenburg, S., Seifert, J., Urbach, H. P., Mosk, A. P., and Coene, W., "Wavelength-multiplexed Multi-mode EUV Reflection Ptychography based on Automatic-Differentiation," *Light: Science and Applications* (in press). arXiv:2311.14780 [physics].